Robust Registration Method of 3D Point Cloud Data

Sungho Suh, Hansang Cho and Donglok Kim
Samsung Electro-Mechanics, 150 Maeyoung-ro, Suwon, Korea

Keywords: Point Cloud, 3D Affine Transformation, Height Map Matching.

Abstract: 3D point cloud data is used for 3D model acquisition, geometry processing and 3D inspection. Registration of 3D point cloud data is crucial for each field. The difference between 2D image registration and 3D point cloud registration is that the latter requires several things to be considered: translation on each plane, rotation, tilt and etc. This paper describes a method of registering 3D point cloud data with noise. The relationship between the two sets of 3D point cloud data can be obtained by Affine transformation. In order to calculate 3D Affine transformation matrix, corresponding points are required. To find the corresponding points, we use the height map which is projected from 3D point cloud data onto XY plane. We formulate the height map matching as a cost function and estimate the corresponding points. To find the proper 3D Affine transformation matrix, we formulate a cost function which uses the relationship of the corresponding points. Also the proper 3D Affine transformation matrix can be calculated by minimizing the cost function. The experimental results show that the proposed method can be applied to various objects and gives better performance than the previous work.

1 INTRODUCTION

The method of image registration is to find a correspondence between the original reference image and the target image. It is used for various pattern recognition, image processing and machine vision tasks including object tracking (Comaniciu et al., 2003), object recognition (Belongie et al., 2002), occlusion handling (Nguyen and Smeulders, 2004), industrial inspection (Rau and Wu, 2005) (Chena et al., 2009), etc. And the method of image registration is also used for 3D model acquisition, geometry processing and 3D inspection. Especially, we consider the registration between CAD data and the input data, or two input data sets which are provided as 3D point cloud data. For 3D scanning, the data inputs are acquired as point cloud data. The acquired data as 3D point cloud data are shown in Figure 1. There is a problem in aligning the input data as point cloud data to the given model.

The difference between 2D image registration and 3D point cloud registration is that the latter requires several things to be considered: translation on every plane, rotation, tilt, etc. The relationship between two 3D point cloud data sets can be obtained by Affine transformation. If the Affine transformation matrix between 3D point cloud data sets is obtained, 3D point cloud data registration can be performed.

There are several popular methods for aligning two point cloud data sets. Some of the most general methods for registration are Iterative Closest Point algorithm (P.J.Besl and McKay, 1992) (Y. and G, 1991) and its variants (Rusinkiewicz and Levoy, 2001). These methods start with two point cloud data sets and refine the transformation between corresponding points iteratively. One of them uses Eucledian distance for measuring the point-to-point distance. This method converges slowly for input point cloud and the given. Another metric uses the point to plane distance. When the initial position is close to the given model and the input data has low noise, it is fast to converge for the given model. However, when the initial position is far from the given model or when the input data is noisy, it cannot find the position. Besides, many enhanced methods of the Iterative Closest Point algorithm propose different error metrics and point selection methods. (G. et al., 1992) (Fitzgibbon, 2003) (Gelfand et al., 2003) (Jost et al., 2003) (Mitra et al., 2004) However, all the methods are slow because of using iterative computation and they are not robust to noise.

In order to solve the problems, we propose a robust registration method of 3D point cloud data. Our method does not use iterative computation and it can find a registration position of two point cloud data sets with noise. To obtain 3D Affine transformation matrix, corresponding points among two point cloud data sets need to be found. To find corresponding points,

Suh, S., Cho, H. and Kim, D.
Robust Registration Method of 3D Point Cloud Data.
DOI: 10.5220/0005750606300637
In *Proceedings of the 5th International Conference on Pattern Recognition Applications and Methods (ICPRAM 2016)*, pages 630-637
ISBN: 978-989-758-173-1

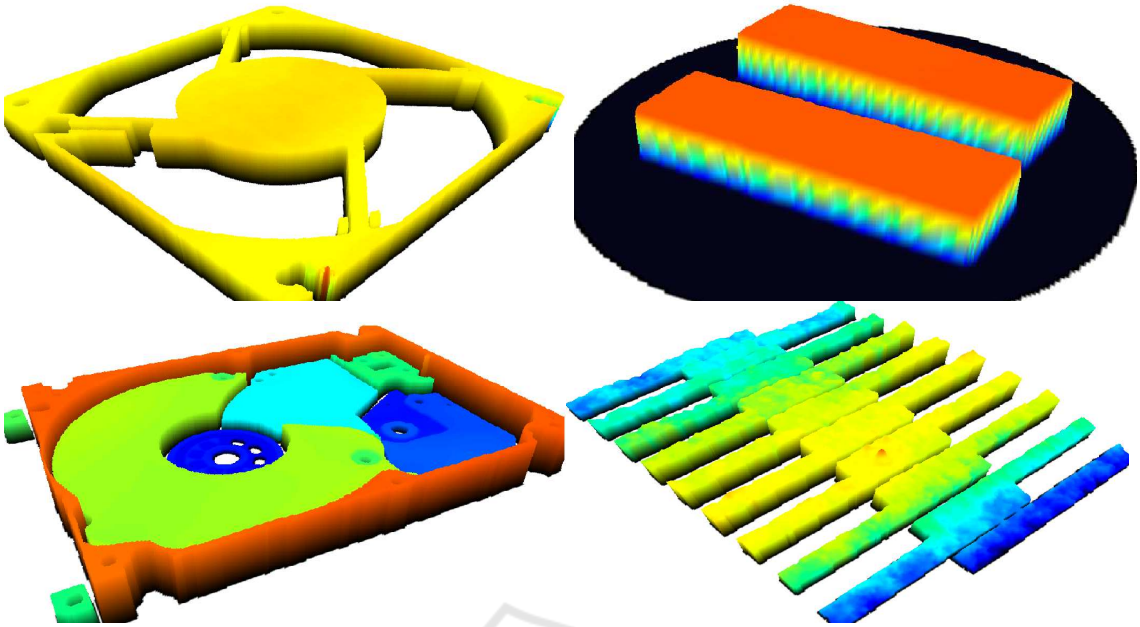

Figure 1: Display 3D point cloud.

we use the height map which is projected from 3D point cloud data onto XY plane. The height map has pixel intensity from the height value of each point. The height map is shown in Figure 2. The net pattern in Figure 2 is caused by the region without point cloud data. Some of the points can be missed and have noise when the point cloud data is obtained by a scanning machine. We need to consider the missed points when we match two height maps which are projected from two 3D point cloud data sets. If the two height maps are matched, corresponding points can be estimated. To match two height maps, the previous work (Suh and Cho, 2015) proposed a 2D height map matching method by calculating 2D Affine transformation matrix, but it can especially be applied to the HDD stamped base inspection (Park et al., 2013). As one of the features of the HDD stamped base, there are multiple circles on the base. To calculate the 2D Affine transformation matrix, it uses circle fitting for corresponding points between two height maps. But it needs the corresponding points of more than three. In other words, it cannot be applied to other objects which do not have any features like circle or have circles less than three.

In this paper, we propose a cost function, which consists of the difference between the intensities of two height maps, for matching two height maps. The corresponding points on the 3D coordinate can be obtained by minimizing the cost function. By using such points, we propose a method designed to achieve 3D Affine transformation matrix. To find the proper 3D Affine transformation matrix, we formulate a cost function which uses the relationship of corresponding points. Also the proper 3D Affine transformation matrix can be calculated by minimizing the cost function. Then the two 3D point cloud data sets can be matched.

The rest of this paper is organized as follows. The details of matching two height maps and 3D registration of 3D point cloud data sets are proposed in Section2. In Section 3, the experimental results are presented. The experiments are performed for three objects including HDD stamped base. The paper concludes in Section 4 with description of our future work.

2 REGISTRATION OF 3D POINT CLOUD DATA SETS

In this section, we first match two height maps by the proposed cost function. And we propose 3D registration method of point cloud data sets based on the result of matching two height maps.

2.1 Matching Two Height Maps on XY-plane

To obtain a 3D Affine transformation matrix between two 3D point cloud data sets, finding corresponding points is needed. First, we express two 3D point cloud sets as two height maps on XY-plane. It means that the resolution is expressed as the distance between

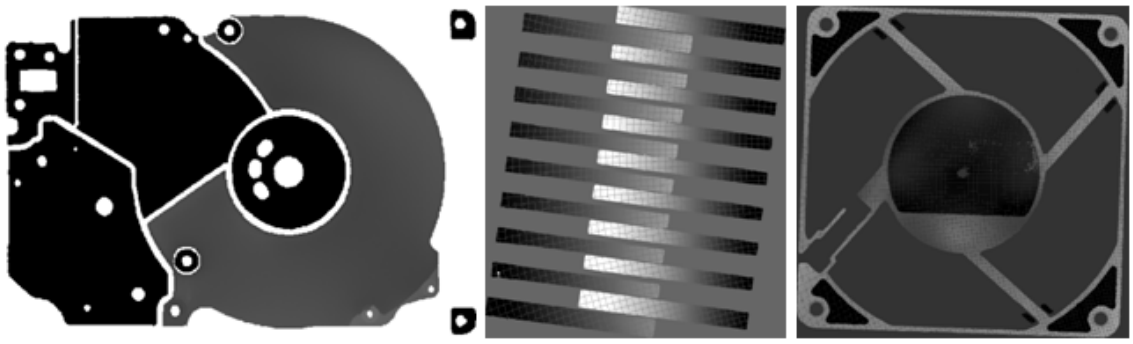

Figure 2: Height maps of 3D point cloud on XY-plane.

x and y points and each pixel value has the height value on Z-axis. There can be errors in translation, scale and rotation errors between those two 2D height maps. The height maps are shown in Figure 2.

We assume that pixel intensities of two height maps, which are height values, have translation and scale errors. We can formulate a cost function as a sum of difference between two height maps.

$$\min_{(d_x,d_y)} \sum_{(x,y)} [\alpha z(x+d_x, y+d_y) + z_0 - w(x,y)]^2 \quad (1)$$

where d_x, d_y are the translation offsets between the two height maps, α is a scale value, z, w are pixel intensities of target and input height maps, and z_0 is a translation offset of height. If the translation offsets which minimize (1) are calculated, corresponding points between two 3D point cloud data sets can be obtained. Furthermore, we assign several template images on the height map and calculate the translation offsets for each template image in order to reduce effects of rotation and computation. We assume for reducing the number of variables that

$$z_0 = \tilde{w} - \alpha\tilde{z} \quad (2)$$

where $\tilde{w}, \tilde{z}$ are average pixel intensities of two height maps. We can rewrite (1) by applying (2).

$$\min_{(d_x,d_y)} [\sum_{(x,y)} \{\alpha(z(x+d_x, y+d_y) - \tilde{z}) - (w(x,y) - \tilde{w})\}^2] \quad (3)$$

(3) can be expanded as follow.

$$\begin{aligned} \min_{(d_x,d_y)} [\sum_{(x,y)} [&\alpha^2 (z(x+d_x, y+d_y) - \tilde{z})^2 \\ &- 2\alpha(z(x+d_x, y+d_y) - \tilde{z})(w(x,y) - \tilde{w}) \\ &+ (w(x,y) - \tilde{w})^2]] \end{aligned} \quad (4)$$

We define the total number of pixels as N, then (4) can be rewritten as follow.

$$\min_{(d_x,d_y)} [N\alpha^2\sigma_z^2 - 2N\alpha\sigma_{zw} + N\sigma_w^2] \quad (5)$$

where σ is standard deviation. To simplify the equation, we assume $\alpha = \frac{\sigma_{zw}^2}{\sigma_z^2}$ and express (5) as

$$\min_{(d_x,d_y)} N\sigma_w^2 (1 - \frac{\sigma_{zw}^2}{\sigma_w^2\sigma_z^2}) \quad (6)$$

In (6), N and σ_w^2 can be removed because they are constant values. Therefore, (6) can be expressed as follow.

$$\max_{(d_x,d_y)} \frac{\sigma_{zw}^2}{\sigma_w^2\sigma_z^2} \quad (7)$$

Through (7), translation offset of each template image can be obtained and the corresponding points between 3D points also can be estimated by matching those two height maps.

2.2 3D Registration of Point Cloud Data Sets

If the corresponding 3D points between the two point cloud data sets are given by the method mentioned in the previous subsection, the corresponding relation is formulated as follow.

$$\begin{bmatrix} u \\ v \\ w \end{bmatrix} = \begin{bmatrix} t_{11} & t_{12} & t_{13} \\ t_{21} & t_{22} & t_{23} \\ t_{31} & t_{32} & t_{33} \end{bmatrix} \begin{bmatrix} x \\ y \\ z \end{bmatrix} + \begin{bmatrix} t_{14} \\ t_{24} \\ t_{34} \end{bmatrix} \quad (8)$$

where (u, v, w) is the coordinate of the target data, (x, y, z) is the corresponding point coordinate on input data to the target data. To obtain unknown components of the Affine transformation matrix above, we propose a cost function as follows.

$$\begin{aligned} \min_{\mathbf{T}} \sum_k [&(t_{11}x_k + t_{12}y_k + t_{13}z_k + t_{14} - u_k)^2 \\ &+ (t_{21}x_k + t_{22}y_k + t_{23}z_k + t_{24} - v_k)^2 \\ &+ (t_{31}x_k + t_{32}y_k + t_{33}z_k + t_{34} - w_k)^2] \end{aligned} \quad (9)$$

where $\mathbf{T}$ is the 3D Affine transformation matrix composed of t, and k is the index of the corresponding point.

As shown above, we obtain the components of the 3D Affine transformation matrix which minimizes the difference between the point on the two 3D point cloud data sets after applying 3D Affine transformation. In order to reduce the number of variables,

$$\begin{aligned} t_{14} &= \tilde{u} - \tilde{x}t_{11} - \tilde{y}t_{12} - \tilde{z}t_{13} \\ t_{24} &= \tilde{v} - \tilde{x}t_{21} - \tilde{y}t_{22} - \tilde{z}t_{23} \\ t_{34} &= \tilde{w} - \tilde{x}t_{31} - \tilde{y}t_{32} - \tilde{z}t_{33} \end{aligned} \tag{10}$$

where $\tilde{x}$, $\tilde{y}$, $\tilde{z}$, $\tilde{u}$, $\tilde{v}$, $\tilde{w}$ are the average of each component. By using (10), (9) can be rewritten as

$$\begin{aligned} \min_{\mathbf{T}} \sum_k [&(t_{11}(x_k - \tilde{x}) + t_{12}(y_k - \tilde{y}) + t_{13}(z_k - \tilde{z}) \\ &-(u_k - \tilde{u}))^2 + (t_{21}(x_k - \tilde{x}) + t_{22}(y_k - \tilde{y}) \\ &+t_{23}(z_k - \tilde{z}) - (v_k - \tilde{v}))^2 + (t_{31}(x_k - \tilde{x}) \\ &+t_{32}(y_k - \tilde{y}) + t_{33}(z_k - \tilde{z}) - (w_k - \tilde{w}))^2] \end{aligned} \tag{11}$$

Thus, we can rewrite (11) as

$$\begin{aligned} F = \min_{\mathbf{T}} \sum_k [&(t_{11}^2\sigma_x^2 + t_{12}^2\sigma_y^2 + t_{13}^2\sigma_z^2 \\ &+ 2t_{11}t_{12}\sigma_{xy} + 2t_{11}t_{13}\sigma_{xz} + 2t_{12}t_{13}\sigma_{yz} \\ &- 2t_{11}\sigma_{xu}] - 2t_{12}\sigma_{yu} - 2t_{13}\sigma_{zu}) + (t_{21}^2\sigma_x^2 \\ &+ t_{22}^2\sigma_y^2 + t_{23}^2\sigma_z^2 + \sigma_v^2 + 2t_{21}t_{22}\sigma_{xy} \\ &+ 2t_{21}t_{23}\sigma_{xz} + 2t_{22}t_{23}\sigma_{yz} - 2t_{21}\sigma_{xv} \\ &- 2t_{22}\sigma_{yz} - 2t_{23}\sigma_{zv}) + (t_{31}^2\sigma_x^2 + t_{32}^2\sigma_y^2 \\ &+ t_{33}^2\sigma_z^2 + \sigma_w^2 + 2t_{31}t_{32}\sigma_{xy} + 2t_{31}t_{33}\sigma_{xz} \\ &+ 2t_{32}t_{33}\sigma_{yz} - 2t_{31}\sigma_{zw} - 2t_{32}\sigma_{yw} - 2t_{33}\sigma_{zw}] \end{aligned} \tag{12}$$

where σ is the standard deviation of each component. All standard deviations can be calculated from the target and input data.

To find the value of t_{ij} that minimizes the cost function (12), we set $\partial F / \partial t_{ij} = 0$. And all of the equations can be written as

$$\begin{aligned} t_{11}\sigma_x^2 + t_{12}\sigma_{xy} + t_{13}\sigma_{xz} - \sigma_{xu} &= 0, \\ t_{12}\sigma_y^2 + t_{11}\sigma_{xy} + t_{13}\sigma_{yz} - \sigma_{yu} &= 0, \\ t_{13}\sigma_z^2 + t_{11}\sigma_{xz} + t_{12}\sigma_{yz} - \sigma_{zu} &= 0, \\ t_{21}\sigma_x^2 + t_{22}\sigma_{xy} + t_{23}\sigma_{xz} - \sigma_{xv} &= 0, \\ t_{22}\sigma_y^2 + t_{21}\sigma_{xy} + t_{23}\sigma_{yz} - \sigma_{yv} &= 0, \\ t_{23}\sigma_z^2 + t_{21}\sigma_{xz} + t_{22}\sigma_{yz} - \sigma_{zv} &= 0, \\ t_{31}\sigma_x^2 + t_{32}\sigma_{xy} + t_{33}\sigma_{xz} - \sigma_{xw} &= 0, \\ t_{32}\sigma_y^2 + t_{31}\sigma_{xy} + t_{33}\sigma_{yz} - \sigma_{yw} &= 0, \\ t_{33}\sigma_z^2 + t_{31}\sigma_{xz} + t_{32}\sigma_{yz} - \sigma_{zw} &= 0 \end{aligned} \tag{13}$$

The system equation problem can be represented in the following matrix form:

$$\begin{aligned} \begin{bmatrix} \sigma_x^2 & \sigma_{xy} & \sigma_{xz} \\ \sigma_{xy} & \sigma_y^2 & \sigma_{yz} \\ \sigma_{xz} & \sigma_{yz} & \sigma_z^2 \end{bmatrix} \begin{bmatrix} t_{11} \\ t_{12} \\ t_{13} \end{bmatrix} &= \begin{bmatrix} \sigma_{xu} \\ \sigma_{yu} \\ \sigma_{zu} \end{bmatrix} \\ \begin{bmatrix} \sigma_x^2 & \sigma_{xy} & \sigma_{xz} \\ \sigma_{xy} & \sigma_y^2 & \sigma_{yz} \\ \sigma_{xz} & \sigma_{yz} & \sigma_z^2 \end{bmatrix} \begin{bmatrix} t_{21} \\ t_{22} \\ t_{23} \end{bmatrix} &= \begin{bmatrix} \sigma_{xv} \\ \sigma_{yv} \\ \sigma_{zv} \end{bmatrix} \\ \begin{bmatrix} \sigma_x^2 & \sigma_{xy} & \sigma_{xz} \\ \sigma_{xy} & \sigma_y^2 & \sigma_{yz} \\ \sigma_{xz} & \sigma_{yz} & \sigma_z^2 \end{bmatrix} \begin{bmatrix} t_{31} \\ t_{32} \\ t_{33} \end{bmatrix} &= \begin{bmatrix} \sigma_{xw} \\ \sigma_{yw} \\ \sigma_{zw} \end{bmatrix} \end{aligned} \tag{14}$$

Here all σ are known parameters. Thus, using (10) and (14), we can obtain all elements of the 3D Affine transformation. The input 3D point cloud data can be aligned to the target 3D point cloud data after applying the obtained the 3D Affine transformation to all of the points on the input data.

3 EXPERIMENTAL RESULT

In this section, we evaluate the performance of the proposed method with artificially transformed data and real data of HDD stamped base. And we compare the results of the proposed method to the results of the previous work. Additionally, we evaluate the performance for the other objects, not HDD stamped base, without circle patterns.

In our experiment, Coherix S150 Holographic Sensor (Christman et al., 2012) is used for acquiring 3D point cloud data. We acquire the 3D point cloud data by the resolution as 0.08 *mm*. First, we transform the CAD data of HDD stamped base to several cases. 1) 1 degree rotated on all planes, 2) 2 degrees rotated on all planes, 3) 3 degrees rotated on all planes, 4) transformed by random transformation matrix. Furthermore, we acquire the 3D point cloud data of five HDD stamped bases. Using those data sets, we compare the previous work (Suh and Cho, 2015) and the proposed method. The results are shown in Figure 3, 4, 5, 6, 7. First left images are the height maps of the original CAD, second left images are input data which are the height maps of the artificially transformed data and scanned data. Third ones and last ones show the example height maps of the result by the previous work (Suh and Cho, 2015) and the proposed method.

In the figures, the results by the proposed method are changed to the height maps of the CAD. And the input data which have rotation and translation on XY-plane are also transformed to the height maps of the CAD. Comparing the results of the proposed method and the results of the previous work which uses the

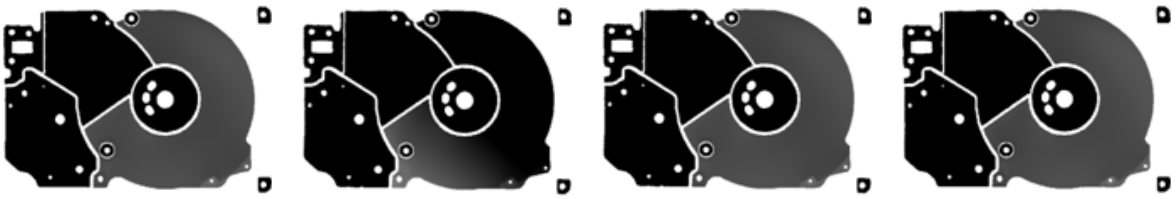

(a) CAD. (b) Input data. (c) By the method in (Suh and Cho, 2015). (d) By the proposed method.

Figure 3: Registration for the data rotated 1 degree on all planes.

(a) CAD. (b) Input data. (c) By the method in (Suh and Cho, 2015). (d) By the proposed method.

Figure 4: Registration for the data rotated 2 degree on all planes.

(a) CAD. (b) Input data. (c) By the method in (Suh and Cho, 2015). (d) By the proposed method.

Figure 5: Registration for the data rotated 3 degree on all planes.

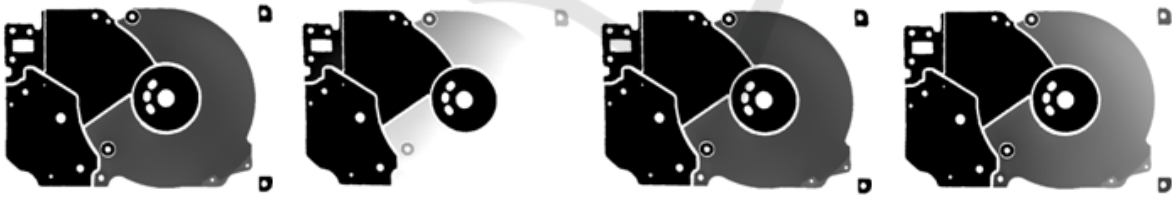

(a) CAD. (b) Input data. (c) By the method in (Suh and Cho, 2015). (d) By the proposed method.

Figure 6: Registration for the data rotated by random transformation matrix.

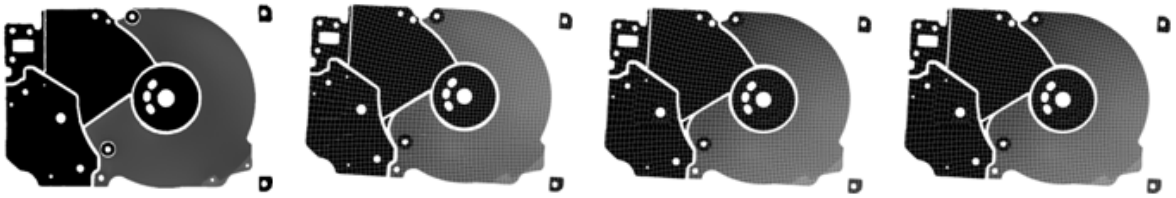

(a) CAD. (b) Input data. (c) By the method in (Suh and Cho, 2015). (d) By the proposed method.

Figure 7: Registration for the real data of HDD stamped base.

Table 1: Average height differences for HDD stamped base data sets.

	By input data	By the previous work	By the proposed method
1° rotated	0.2149	0.0039	0.0155
2° rotated	0.3647	0.0088	0.0162
3° rotated	0.4690	0.0229	0.0159
transformed randomly	0.5721	0.1202	0.0097
Real data	1.1145	0.1701	0.0953

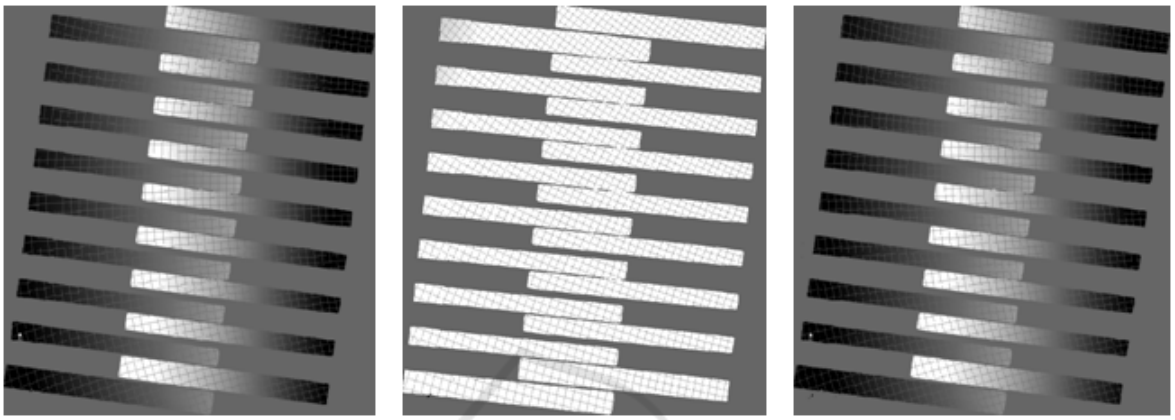

(a) Target data (b) Input data. (c) By the proposed method.

Figure 8: Registration for Pin.

center points of circle feature, both methods make the input data transformed to the CAD data as well. To measure the defined error, we compare height differences between the original CAD data and the methods. The height differences are shown in Table 1.

Table 1 shows the averages of height difference for HDD stamped base data sets. The differences are represented as *mm*. Both the previous work and the proposed method make the input data sets converged to the CAD data, because the averages are close to 0. And the results of the proposed method are similar to the results of the previous work. The result of the proposed method for the data randomly transformed reduces errors dramatically compared to the result of the previous work. And using the input data which has bigger error, the proposed method gives better performance than the previous work. In addition, the resolution of the 3D point cloud data is $0,08mm$ in the experiment as mentioned earlier. The height errors of the proposed method are almost less than 0.08. It means that the error is within 1 pixel and it is within error range. However, the previous method shows the errors for the data transformed randomly and the real data are much larger than 0.08. Therefore, we claim that the proposed method allows the 3D point cloud data of HDD stamp base to be aligned to the CAD data more accurately than the previous method.

We also acquire the 3D point cloud data sets of the other objects and show the results of the proposed method with the data sets. Figure 8 and 9 show the height map of the 3D point cloud data for rib cage shaped metal object and CPU fan. In the figures, even though there are big differences between the target and input data sets, the results of the proposed method show that the proposed method makes the input data sets transform to the target data sets as well. As same as Table 1, Table 2 shows the average height differences for the two objects.

Table 2: Average height differences for metal pin and CPU fan.

	Input data	By the Proposed method
PIN	1.3143	0.0174
FAN	1.2364	0.0732

The method in (Suh and Cho, 2015) cannot be applied to the objects because the objects do not have enough circle features for circle fitting. Also, since the resolution is $0.08mm$ for the data sets and the height errors by the proposed method in Table 2 are less than $0.08mm$, the proposed method can perform the registration of 3D point cloud data for various objects properly.

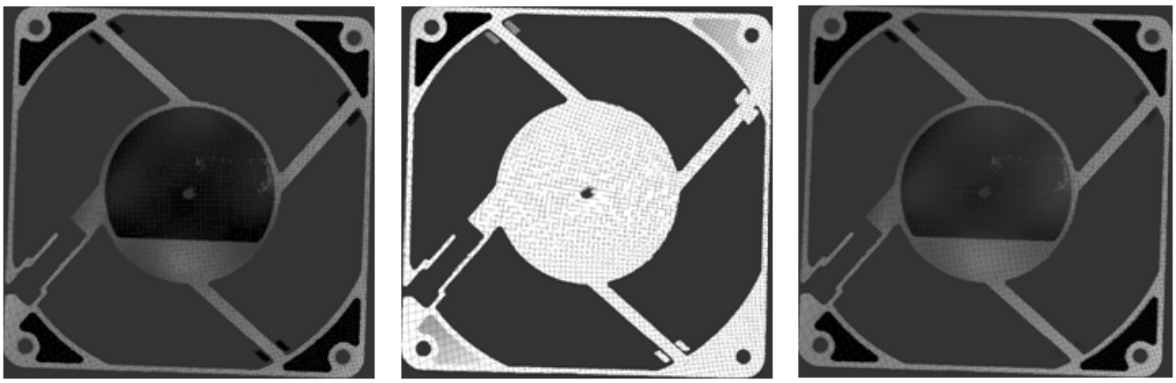

(a) Target data. (b) Input data. (c) By the method in (Suh and Cho, 2015).

Figure 9: Registration for Fan.

4 CONCLUSIONS

In this paper, a robust registration method has been proposed for 3D point cloud data with noise. The proposed method is robust to noise and do not use iterative computation. The proposed method can apply for the objects without any circular features. The proposed method generated the height map, whose pixel intensity is represented as the height value of the 3D point cloud data, and matched the two height maps from two different 3D point cloud data sets. In order to match the two height maps, we proposed a cost function and found translation offsets for template images. The corresponding points between the two 3D point cloud data sets can be obtained from the matched two height maps. We formulated another cost function for calculating the components of 3D Affine transformation matrix by using the corresponding points from height map matching. We used 3D point cloud data sets of HDD stamp base and the other objects for a performance evaluation. The experiment result showed that the proposed method gave better performance than the previous work (Suh and Cho, 2015) for HDD stamp base and could be applied to the other objects without circle features.

Since the experiment was performed for three different objects, we need to experiment more various objects. Moreover, the performance of the height map matching method can differ how to select the template images. Therefore, further investigation is needed to select proper template images automatically.

REFERENCES

Belongie, S., Malik, J., and Puzicha, J. (2002). Shape matching and object recognition using shape contexts. *IEEE Transations on Pattern Analysis and Machine Intelligence*, 24(24):509 – 522.

Chena, C.-S., Yeha, C.-W., and Yin, P.-Y. (2009). A novel Fourier descriptor based image alignment algorithm for automatic optical inspection. *Journal of Visual Communication and Image Representation*, 20:178–189.

Christman, S., Doman, D., and Kamal, A. S. B. A. (2012). Final report for a demonstration structure for a 3d holographic sensor. *University of Michigan ME450*.

Comaniciu, D., Ramesh, V., and Meer, P. (2003). Kernel-based object tracking. *IEEE Transations on Pattern Analysis and Machine Intelligence*, 25(5):564 – 577.

Fitzgibbon, A. W. (2003). Robust registration of 2d and 3d point sets. *Image and Vision Computing*, 21:1145–1153.

G., C., S., L., R., S., and L., B. (1992). From accurate range imaging sensor calibration to accurate model-based 3d object localization. *IEEE Conference of Computer Vision and Pattern Recognition*, pages 83–89.

Gelfand, N., Ikemoto, L., Rusinkiewicz, S., and Levoy, M. (2003). Geometrically stable sampling for the icp algorithm. *3-D Digital Imaging and Modeling*, pages 260–267.

Jost, Timothee, and Hugli., H. (2003). A multi-resolution icp with heuristic closest point search for fast and robust 3d registration of range images. *3-D Digital Imaging and Modeling*, pages 427–433.

Mitra, N. J., Gelfand, N., Pottmann, H., and Guibas, L. (2004). Registration of point cloud data from a geometric optimization perspective. *Eurographics/ACM SIGGRAPH symposium on Geometry processing*, pages 22–31.

Nguyen, H. T. and Smeulders, A. W. (2004). Fast Occluded Object Tracking by a Robust Appearance Filter. *IEEE Transations on Pattern Analysis and Machine Intelligence*, 26(8):1099–1104.

Park, K.-S., Lee, H.-C., Kim, J.-H., Kim, S., Seo, J., Rhim, Y., and Park, N.-C. (2013). Analysis on the characteristics of stamped base for 2.5 in hdd. *IEEE Transaction on Magnetics*, 49.

P.J.Besl and McKay, N. (1992). A method for registration

of 3-d shapes. *IEEE Trans. Pattern Analysis and Machine Intelligence*, 14:239–256.

Rau, H. and Wu, C.-H. (2005). Automatic optical inspection for detecting defects on printed circuit board inner layers. *The International Journal of Advanced Manufacturing Technology*, 1(9-10).

Rusinkiewicz, S. and Levoy, M. (2001). Efficient variants of the icp algorithm. *International Conference on 3D Digital Imaging and Modeling*, pages 145–152.

Suh, S. and Cho, H. (2015). Registration of point cloud data for hdd stamped base inspection. *SPIE Optical Engineering+ Applications. International Society for Optics and Photonics*, pages 95991P–95991P–10.

Y., C. and G, M. (1991). Object modeling by registration of multiple range images. *IEEE Conference on Robotics and Automation*.